Sensorless Control of Synchronous Reluctance Motor Drives Based on the TLS EXIN Neuron

Yong-Chao Liu[1], Salah Laghrouche[1], Abdoul N'Diaye[1], Siwan Narayan[2], Giansalvo Cirrincione[3], Maurizio Cirrincione[2]
[1]Energy Department, FEMTO-ST Institute, National Center for Scientific Research (CNRS), UTBM, Université Bourgogne Franche-Comté, Belfort, France
[2]School of Engineering and Physics, University of the South Pacific, Laucala Campus, Suva, Fiji
[3]Department of Electrical Engineering, University of Picardie "Jules Verne", Amiens, France
cn.yong-chao.liu@ieee.org, salah.laghrouche@utbm.fr, abdoul-ousman.n-diaye@utbm.fr, siwan.narayan@usp.ac.fj; exin@u-picardie.fr; maurizio.cirrincione@usp.ac.fj

***Abstract*—This paper proposes a rotor speed and position estimation scheme for the synchronous reluctance motor (SynRM) drive system based on its active flux model in the stator reference frame and the total least squares (TLS) EXIN neuron. Firstly, the active flux model of the SynRM in the stator reference frame is reconstructed to the overdetermined matrix equations. On the basis of that, the estimation of the rotor speed of the SynRM is transferred into solving a TLS problem. The TLS EXIN neuron, which is a recursive TLS algorithm, is used to solve this problem online to extract the rotor speed. The estimated rotor position is obtained from the estimated rotor speed based on the integrator. The feasibility and effectiveness of the proposed rotor speed estimation scheme have been verified by the simulation results.**

Keywords—synchronous reluctance motor, sensorless control, active flux, linear neural networks, total least-squares

I. INTRODUCTION

Over the years, research on the synchronous reluctance motor (SynRM) has attracted much attention because of its magnetless and windingless rotor structure which is low-cost and simple for manufacturing [1]-[8]. The SynRM drive system with high-performance control strategies is considered as a potential alternative to the induction motor (IM) drive system and the permanent-magnet synchronous motor (PMSM) drive system in some industrial applications [2]-[5]. The acquisition of the accurate rotor positon information is the base of many high-performance control schemes of the SynRM drive system [6]-[8]. In general, the mechanical sensor is used to extract the rotor positon information. However, there are several disadvantages of installing this type of sensor, such as increased cost and reliability problem [9]. To further reduce the costs and increase the reliability of the drive system, the rotor-positon-sensorless SynRM drive system is preferred. Thus, the reliable rotor speed and positon estimation scheme for the SynRM drive system should be developed [10]-[20].

As a type of three-phase AC synchronous motors, the sensorless control schemes for SynRM drive system can be divided into two categories: the saliency-based schemes and the model-based schemes [10]-[20]. For the saliency-based schemes, the rotor anisotropic structure is exploited [10]-[13]. The high-frequency rotating voltage signal injection scheme and the high-frequency pulsating voltage signal injection scheme are the two most popular saliency-based schemes [11]-[13]. This category of the estimation scheme is the viable sensorless control scheme at zero and low speeds. For the medium- and high-speed sensorless control, the model-based schemes are adopted [14]-[20]. Just as theirs name implies, these schemes are based on some specific terms in the mathematical model of the SynRM for extracting the rotor speed and position. There are several mathematical model of the SynRM can be used to design rotor speed and position estimation schemes. In the stator reference frame, the extended electromotive force (EEMF) model, which the EEMF terms are used to extract the rotor positon, and the active flux model, which the acquisition of the rotor position depends on the active flux terms or theirs derivatives, are two popular choices [16]-[18]. To estimate the EEMF, the active-flux terms or theirs derivatives, some model-based rotor speed and position estimation schemes for SynRM drive system have been designed [18]-[20], such as the disturbance observers [18], the sliding-mode observers [19], and the adaptive full-order observers [20]. However, the above-mentioned model-based schemes are a type of indirect estimation schemes. They usually need the phase-locked loop or trigonometric function calculation to extract the rotor speed and position form the estimated speed-related terms [18]-[20].

Apart from the indirect estimation schemes, the linear-neural-network-based schemes that directly estimate the rotor speed has been introduced to AC motor drive systems [21]-[26]. In this type of sensorless control scheme, some specific mathematical models of the AC motors are reconstructed to the overdetermined matric equations. Based on that, the rotor speed estimation is transferred to searching the solution of the total least-square (TLS) problem. The so-called TLS EXIN neuron, which is the best recursive algorithm for solving the TLS problem online [27], is used to obtain the TLS solution, namely the estimated rotor speed. For the IM drive system, this neuron-based method has been used to improve the performance of the sensorless control system based on the model reference adaptive system, the adaptive full-order observer and the reduced-order observer [21]-[25], where the rotor flux equations of the IM in the stator reference frame are used to build the overdetermined matrix equations. For the PMSM drive system, this neuron-based method have been also used to achieve sensorless control based on the stator voltage equations in the stator reference

978-1-5386-9350-6/19/$31.00 ©2019 IEEE

frame [26]. However, to the best of the authors' knowledge, no published paper introduces this type of neuron-based method to the sensorless control of the SynRM drive system.

In this paper, based on the active flux model of the SynRM in the stator reference frame, a rotor speed and position estimator for the SynRM drive system with the TLS EXIN neuron is proposed. At first, the overdetermined matrix equations whose solution is the rotor speed are derived from the active flux model of the SynRM in the stator reference frame. From that, the rotor speed is estimated online by the TLS EXIN neuron. The estimated rotor position is obtained from the estimated rotor speed based on the integrator. Simulation results are provided to validate the proposed estimation scheme..

II. Active Flux Model of the SynRM in the Stator Reference Frame

The stator flux equations of the SynRM in the rotor reference frame, namely the *dq*-frame, can be expressed as follows.

$$\begin{bmatrix}\lambda_d\\ \lambda_q\end{bmatrix}=\begin{bmatrix}L_d & 0\\ 0 & L_q\end{bmatrix}\begin{bmatrix}i_d\\ i_q\end{bmatrix} \tag{1}$$

where λ_d and λ_q are the *d*- and *q*-axis components of the stator flux, respectively; i_d and i_q are the *d*- and *q*-axis components of the stator current, respectively; L_d and L_q are the *d*- and *q*-axis synchronous inductances.

Based on (1), the relationship between the active flux and the stator flux of the SynRM in the rotor reference frame can be expressed as follows [16].

$$\begin{bmatrix}\lambda_{ad}\\ \lambda_{aq}\end{bmatrix}=\begin{bmatrix}\lambda_d\\ \lambda_q\end{bmatrix}-L_q\begin{bmatrix}i_d\\ i_q\end{bmatrix}=\begin{bmatrix}\left(L_d-L_q\right)i_d\\ 0\end{bmatrix} \tag{2}$$

where λ_{ad} and λ_{aq} are the *d*- and *q*-axis components of the active flux, respectively.

The stator voltage equations of the SynRM in the rotor reference frame can be expressed as follows.

$$\begin{bmatrix}u_d\\ u_q\end{bmatrix}=R_s\begin{bmatrix}i_d\\ i_q\end{bmatrix}+p\begin{bmatrix}\lambda_d\\ \lambda_q\end{bmatrix}+\begin{bmatrix}0 & -\omega_r\\ \omega_r & 0\end{bmatrix}\begin{bmatrix}\lambda_d\\ \lambda_q\end{bmatrix} \tag{3}$$

where u_d and u_q are the *d*- and *q*-axis components of the stator voltage, respectively; R_s is the stator resistance, ω_r is the rotor electrical speed, and p is the differential operator.

Based on (1) and (2), (3) can be rewritten as follows.

$$\begin{bmatrix}u_d\\ u_q\end{bmatrix}=\begin{bmatrix}R_s+pL_q & -\omega_r L_q\\ \omega_r L_q & R_s+pL_q\end{bmatrix}\begin{bmatrix}i_d\\ i_q\end{bmatrix}+\begin{bmatrix}p\lambda_{ad}\\ \omega_r\lambda_{ad}\end{bmatrix} \tag{4}$$

Transferring (4) into the stator reference frame, namely the $\alpha\beta$-frame, and then, substituting (2) into it, the active flux model of the SynRM in the stator reference frame is derived as follows.

$$\begin{aligned}\begin{bmatrix}u_\alpha\\ u_\beta\end{bmatrix}&=\begin{bmatrix}R_s+pL_q & 0\\ 0 & R_s+pL_q\end{bmatrix}\begin{bmatrix}i_\alpha\\ i_\beta\end{bmatrix}\\&+\left(L_d-L_q\right)pi_d\begin{bmatrix}\cos\theta_r\\ \sin\theta_r\end{bmatrix}+\omega_r\left(L_d-L_q\right)i_d\begin{bmatrix}-\sin\theta_r\\ \cos\theta_r\end{bmatrix}\end{aligned} \tag{5}$$

where u_α and u_β are the α- and β-axis components of the stator voltage, respectively; i_α and i_β are the α- and β-axis components of the stator current, respectively; θ_r is the rotor electrical position.

III. Proposed Speed and Position Estimation Scheme Based on the TLS EXIN Neuron

A. Overdetermined Matrix Equation Construction

According to (5), the active flux model of the SynRM in the stator reference frame can be reconstructed to the following overdetermined matrix equations.

$$\begin{aligned}&\begin{bmatrix}-\left(L_d-L_q\right)i_d\sin\theta_r\\ \left(L_d-L_q\right)i_d\cos\theta_r\end{bmatrix}\omega_r=\\&\qquad\begin{bmatrix}u_\alpha-R_s i_\alpha-L_q pi_\alpha-\left(L_d-L_q\right)pi_d\cos\theta_r\\ u_\beta-R_s i_\beta-L_q pi_\beta-\left(L_d-L_q\right)pi_d\sin\theta_r\end{bmatrix}\end{aligned} \tag{6}$$

Based on the first-order backward Euler method, the discrete-time form of (5) can be derived as

$$\begin{bmatrix}a_1\\ a_2\end{bmatrix}\omega_r(k)=\begin{bmatrix}b_1\\ b_2\end{bmatrix} \tag{7}$$

where

$$a_1=-\left(L_d-L_q\right)i_d(k)\sin\theta_r(k-1)$$

$$a_2=\left(L_d-L_q\right)i_d(k)\cos\theta_r(k-1)$$

$$\begin{aligned}b_1=&u_\alpha(k)-R_s i_\alpha(k)-L_q\left(\frac{i_\alpha(k)-i_\alpha(k-1)}{T_s}\right)\\&-\left(L_d-L_q\right)\left(\frac{i_d(k)-i_d(k-1)}{T_s}\right)\cos\theta_r(k-1)\end{aligned}$$

$$\begin{aligned}b_2=&u_\beta(k)-R_s i_\beta(k)-L_q\left(\frac{i_\beta(k)-i_\beta(k-1)}{T_s}\right)\\&-\left(L_d-L_q\right)\left(\frac{i_d(k)-i_d(k-1)}{T_s}\right)\sin\theta_r(k-1)\end{aligned}$$

with the sampling period T_s.

B. Least-Squares Problem Analysis

Equation (7) is written as the form $\boldsymbol{A}\,\omega_r(k)\approx\boldsymbol{b}$, where $\boldsymbol{A}$ and $\boldsymbol{b}$ are named as the data and observation vectors, respectively [27]. For these discrete-time overdetermined equations, the solution can be obtained by the least-squares methods. There are three types of least-square methods: the ordinary least-squares (OLS) method, data least-squares (DLS) method and the TLS method. The OLS method is based on the assumption that the

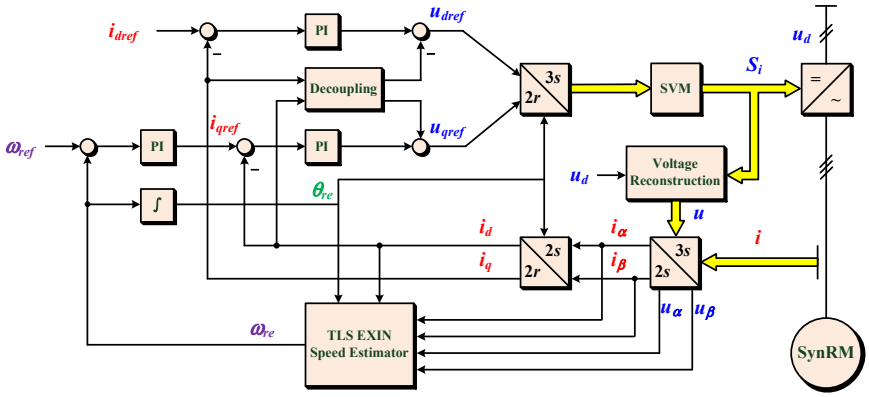

Fig. 1. Signal flow graph of the proposed sensorless strategy based on the TLS EXIN neuron.

errors are present only in the observation vector, while the DLS method is used for the problem that the errors only exist in the data vector. The solution for the OLS problem and DLS problem are obtained by minimizing the following cost functions $E_{OLS}(\omega_r)$ and $E_{DLS}(\omega_r)$, respectively.

$$E_{OLS}(\omega_r) = (\boldsymbol{A}\omega_{re} - \boldsymbol{b})^T (\boldsymbol{A}\omega_{re} - \boldsymbol{b}) \tag{8}$$

$$E_{DLS}(\omega_r) = \frac{(\boldsymbol{A}\omega_r - \boldsymbol{b})^T (\boldsymbol{A}\omega_r - \boldsymbol{b})}{\omega_r^2} \tag{9}$$

As shown in (7), the data vector is based on the *d*-axis component of the measured stator current and the estimated rotor electrical position obtained from the integral of the estimated rotor electrical speed; while the observation vector is composed of the calculated α- and β-axis components of the measured stator voltage, the α-, β-, and *d*-axis components of the measured stator current as well as the estimated rotor electrical position. Thus, it can be observed that both data and observation vectors are affected by errors and noises. For these reasons, solving the overdetermined matrix equations (7) is a TLS problem, which based on the assumption that both data and observation vectors are affected by the errors, rather than an OLS problem or a DLS problem. The solution for the TLS problem is obtained by minimizing the following cost function $E_{TLS}(\omega_r)$.

$$E_{DLS}(\omega_r) = \frac{(\boldsymbol{A}\omega_r - \boldsymbol{b})^T (\boldsymbol{A}\omega_r - \boldsymbol{b})}{\omega_r^2 + 1} \tag{10}$$

C. The TLS EXIN Neuron

To obtain the TLS solution for (10), based on the gradient descent method, the following TLS EXIN learning law can be adopted [27].

$$\begin{aligned}\omega_{re}(k+1) = \omega_r(k) - \alpha(k)\boldsymbol{\gamma}^T(k)\boldsymbol{A}(k) \\ + \left[\alpha(k)\boldsymbol{\gamma}^T(k)\boldsymbol{\gamma}(k)\right]\omega_{re}(k)\end{aligned} \tag{11}$$

where $\omega_e(k)$ is the estimated rotor electrical speed, $\alpha(k)$ is the positive learning rate, $\boldsymbol{\gamma}(k)$ and $\boldsymbol{\delta}$(k) are defined as

$$\boldsymbol{\gamma}(k) = \frac{\boldsymbol{\delta}(k)}{1 + \omega_{re}^2(k)} \tag{12}$$

$$\boldsymbol{\delta}(k) = \frac{\boldsymbol{A}(k)\omega_{re}(k) - \boldsymbol{b}(k)}{1 + \omega_{re}^2(k)} \tag{13}$$

As proven in [27], $\omega_e(k) = 0$ belongs to the convergence domain of the TLS. Therefore, the initial value $\omega_e(0)$ is set to 0 to ensure the convergence of the solution in this paper.

D. Main Control Structure

As shown in Fig. 1, the constant i_d control strategy, which is most natural for the SynRM drive system [28], is selected as the main control structure in this paper. This control strategy is carried out in the rotor reference frame. For the direct axis, the reference value of direct axis component of stator current i_{dref} is set to a constant value in the inner direct axis stator current loop. For the quadrature axis, the outer speed loop whose real speed information comes from the speed estimator based on the TLS EXIN neuron controls the inner quadrature axis loop. All three control loops are based on the proportional-integral controllers. The rotor electrical position for the frame transformation is obtained by integrating estimated rotor electrical speed. In addition, the stator phase voltage for the speed estimator are calculated based on the dc-link voltage and the duty cycles of the inverter.

IV. Simulation Results

The proposed TLS-EXIN-neuron-based sensorless control scheme for the SynRM drive system is tested with the MATLAB/Simulink-based simulation. The system parameters are listed as follows: rated power is 2 kW, rated current is 5.4 A, dc-bus voltage is 650 V, rated torque is 12.4 N·m, rated rotor mechanical speed is 1500 rpm, the rotor inertia is 7.8 x 10^{-3} kg·m^2, R_s is 1.85 Ω, L_d is 218 mH, L_q is 34.1 mH, T_s is 1 x 10^{-5} s, switching frequency is 5000 Hz.

In the first test, the value of i_{dref} is kept at 3.8 A and the load is set at 5 N·m. The reference rotor mechanical speed steps form 500 rpm to 1000 rpm at 2.0 s, and steps again from 1000 rpm to 1500 rpm at 4.0 s. Fig. 2 shows the measured i_d, the measured

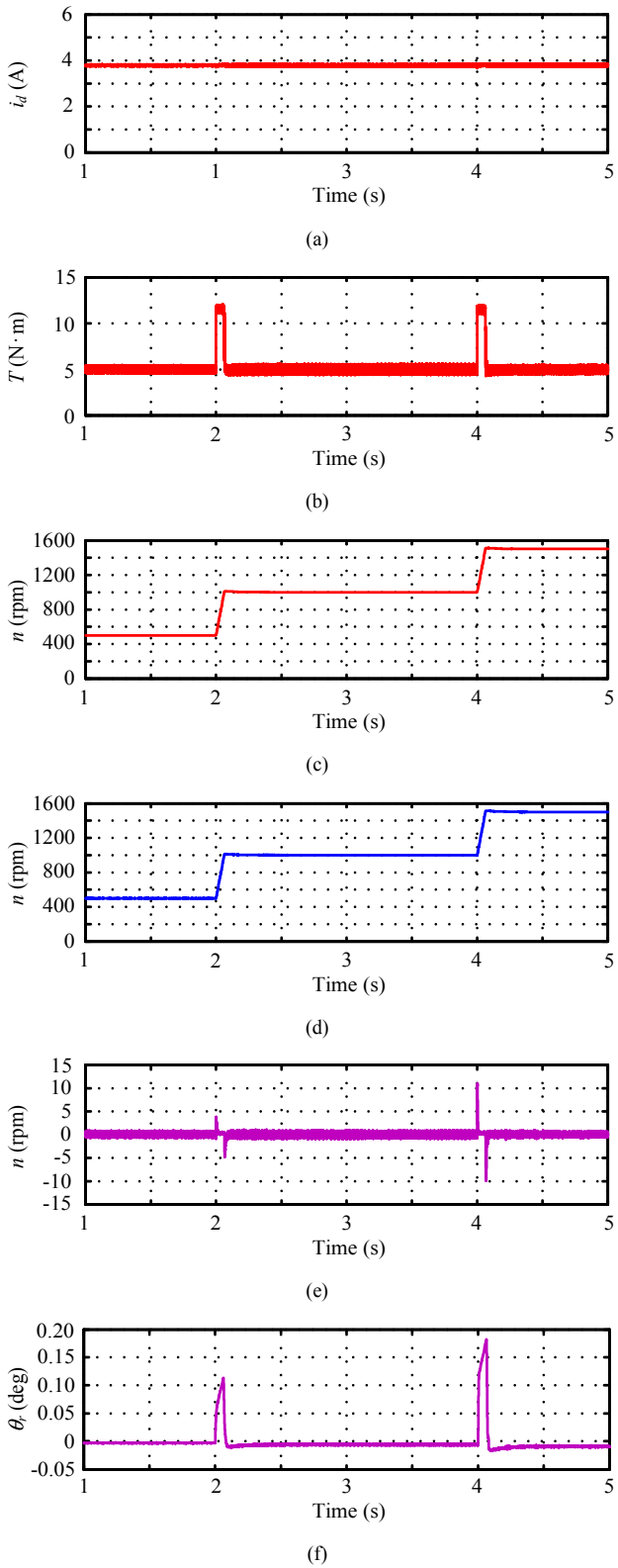

Fig. 2. Simulation results of the first test. (a) Measured i_d, (b) measured torque, (c) measured rotor mechanical speed, (d) estimated rotor mechanical speed, (e) rotor mechanical speed error, and (f) rotor mechanical position error.

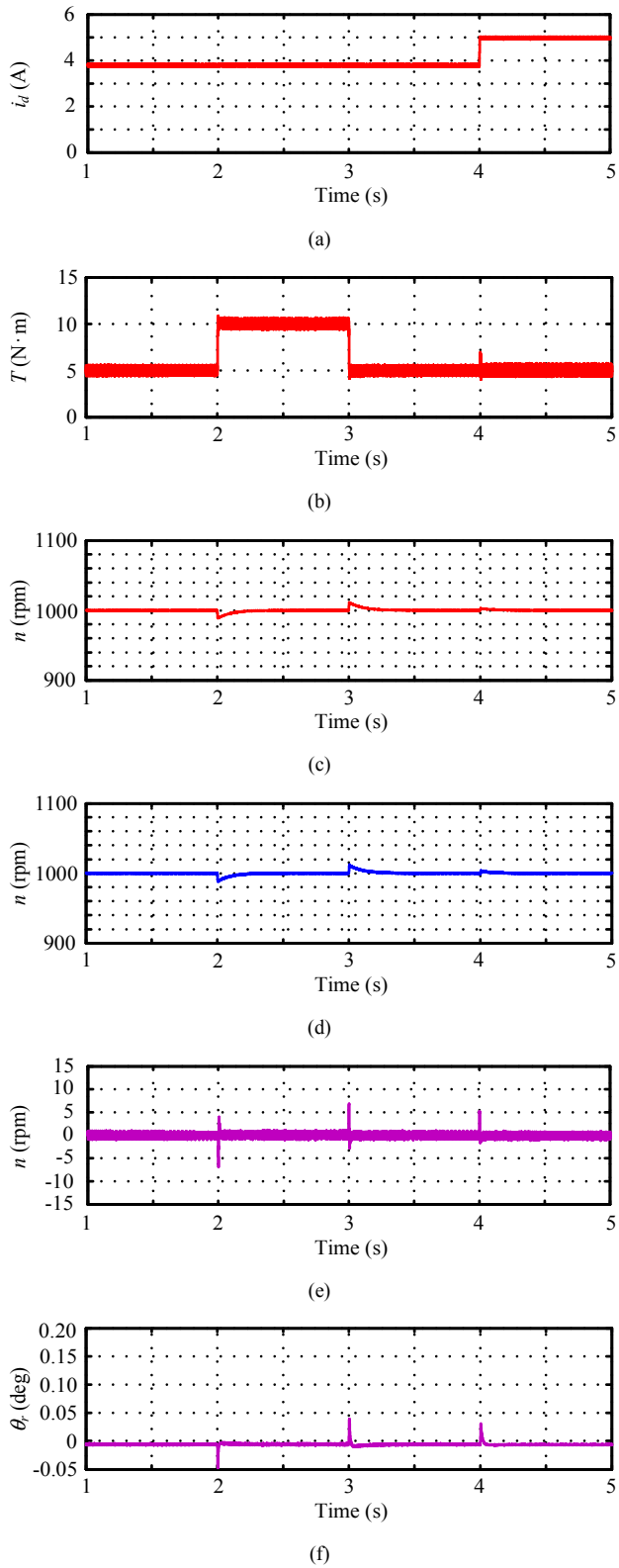

Fig. 2. Simulation results of the second test. (a) Measured i_d, (b) measured torque, (c) measured rotor mechanical speed, (d) estimated rotor mechanical speed, (e) rotor mechanical speed error, and (f) rotor mechanical position error.

torque, the measured rotor mechanical speed, the estimated rotor mechanical speed, the mechanical rotor speed and position errors. It can be seen that the estimated mechanical speed tracks the reference value well and the rotor speed and positions errors are acceptable.

In the second test, the reference rotor mechanical speed is kept at 1000 rpm. The load steps from 5 N·m to 10 N·m at 2.0 s and declines to 5.0 N·m at 3.0 s. The value of i_{dref} steps from 3.8 A to 5.0 A at 4.0 s. the measured i_d, the measured torque, the measured rotor mechanical speed, the estimated rotor mechanical speed, the mechanical rotor speed and position errors are illustrated in Fig. 3. It can be observed that the drive system operates stably and estimated rotor mechanical speed and position errors are also acceptable.

V. CONCLUSIONS

This paper proposes a rotor speed and position estimator for the sensorless-constant-i_d-controlled SynRM drives based on the active flux model of the SynRM and the TLS EXIN neuron. The rotor speed estimation is considered as a TLS problem solved online by the TLS EXIN neuron. The calculated stator voltage components, measured stator current components and the estimated rotor electrical position are received as inputs of the TLS EXIN neuron, and the estimated rotor electrical speed is provided as outputs of the TLE EXIN neuron. Based on an integrator, the rotor electrical position is also extracted from the estimated rotor electrical speed. Simulation results have shown the validity and feasibility of the proposed estimation scheme

ACKNOWLEDGMENT

This work was supported by the USP-SRT Research Project: Advanced Control of Synchronous Reluctance Motors for Electrical Vehicles (ACOSREV).

REFERENCES

[1] G. Pellegrino, T. M. Jahns, N. Bianchi, W. L. Soong, and F. Cupertino, The Rediscovery of Synchronous Reluctance and Ferrite Permanent Magnet Motors. Basel: Springer, 2016.

[2] G. Eason, B. Noble, and I. N. Sneddon, "Theoretical and experimental reevaluation of synchronous reluctance machine," *IEEE. Trans. Ind. Electron.*, vol. 57, no. 1, pp. 6-13, Jan. 2010.

[3] N. Bianchi, S. Bolognani, E. Carraro, M. Castiello, and E. Fornasiero, "Electric vehicle traction based on synchronous reluctance motors," *IEEE Trans. Ind. Appl.*, vol. 52, no. 6, pp. 4762–4769, Nov./Dec. 2016.

[4] J. -D. Park, C. Kalev, and H. F. Hofmann, "Control of high-speed solid-rotor synchronous reluctance motor/generator for flywheel-based uninterruptible power supplies," *IEEE Trans. Ind. Electron.*, vol. 55, no. 8, pp. 3038–3046, Aug. 2008.

[5] Y. Wang, and N. Bianchi, "Investigation of self-excited synchronous reluctance generators," *IEEE Trans. Ind. Appl.*, vol. 54, no. 2, pp. 1360–1369, Mar./Apr. 2018.

[6] M. -Y. Wei, and T. -H. Liu, "Design and implementation of an online tuning adaptive controller for synchronous reluctance motor drives," *IEEE Trans. Ind. Electron.*, vol. 60, no. 9, pp. 3644–3657, Sep. 2013.

[7] H. Hadla, and S. M. A. Cruz, "Predictive stator flux and load angle control of synchronous reluctance motor drives operating in a wide speed range," *IEEE Trans. Ind. Electron.*, vol. 64, no. 9, pp. 6950–6959, Sep. 2017.

[8] S. Yamamoto, H. Hirahara, J. B. Adawey, T. Ara, and K. Matsuse, "Maximum efficiency drives of synchronous reluctance motors by a novel loss minimization controller with inductance estimator," *IEEE Trans. Ind. Appl.*, vol. 49, no. 6, pp. 2543–2551, Nov./Dec. 2013.

[9] M. Cirrincione, M. Pucci, and G. Vitale, Power Converters and AC Electrical Drives with Linear Neural Networks. New York: Taylor &Francis, 2012.

[10] F. Briz, M. W. Degner, P. García, and R. D. Lorenz, "Comparison of saliency-based sensorless control techniques for AC machines," *IEEE. Trans. Ind. Appl.*, vol. 40, no. 4, pp. 1107-1115, Jul./Aug. 2004.

[11] M. J. Corley, and R. D. Lorenz, "Rotor position and velocity estimation for a salient-pole permanent magnet synchronous machine at standstill and high speeds," *IEEE. Trans. Ind. Appl.*, vol. 34, no. 4, pp. 784-789 Jul./Aug. 1998.

[12] J. -H. Jang, S. -K. Sul, J. I. Ha, K. Ide, and M. Sawamura, "Sensorless drive of surface-mounted permanent-magnet motor by high-frequency signal injection based on magnetic saliency," *IEEE. Trans. Ind. Appl.*, vol. 39, no. 4, pp. 1031-1039, Jul./Aug. 2003.

[13] Y. -D. Yoon, S. -K. Sul, S. Morimoto, and K. Ide, "High-bandwidth sensorless algorithm for AC machines based on square-wave-type voltage injection," *IEEE. Trans. Ind. Appl.*, vol. 47, no. 3, pp. 1361-1370, May/Jun. 2011.

[14] T. Tuovinen, and M. Hinkkanen, "Adaptive full-order observer with high-frequency signal injection for synchronous reluctance motor drives," *IEEE J. Emerg. Sel. Topics Power Electron.*, vol. 2, no. 2, pp. 181-189, Jun. 2014.

[15] T. Tuovinen, M. Hinkkanen, L. Harnefors, and J. Luomi, "Comparison of a reduced-order observer and a full-order observer for sensorless synchronous motor drives," *IEEE. Trans. Ind. Appl.*, vol. 48, no. 6, pp. 1959-1967, Nov./Dec. 2012.

[16] I. Boldea, M. C. Paicu, G. D. Andreescu, and S.C. Agarlita, "Active flux concept for motion-sensorless unified ac drives," *IEEE. Trans. Power Electron.*, vol. 23, no. 5, pp. 2612-2618, May 2008.

[17] S. -C. Agarlita, I. Boldea, and F. Blaabjerg, "High-frequency- injection-assisted "active-flux"-based sensorless vector control of reluctance synchronous motors, with experiments from zero speed," *IEEE. Trans. Ind. Appl.*, vol. 48, no. 6, pp. 1931-1939, Nov./Dec. 2012.

[18] S. Ichikawa, M. Tomita, S. Doki, and S. Okuma, "Sensorless control of synchronous reluctance motors based on extended EMF models considering magnetic saturation with online parameter identification," *IEEE. Trans. Ind. Appl.*, vol. 42, no. 5, pp. 1264-1274, Sep./Oct. 2006.

[19] Y. -C. Liu, S. Laghrouche, A. N'Diaye, and M. Cirrincione, "Active-flux-based super-twisting sliding mode observer for sensorless vector control of synchronous reluctance motor drives," in *Proc. 7th IEEE Int. Conf. on Renewable Energy Research and Applications*, Paris, 2018, pp. 402-406.

[20] A. Shinke, M. Hasegawa, and K. Matsui, "Torque estimation for synchronous reluctance motors using robust flux observer to magnetic saturation," in *Proc. 2009 IEEE Int. Symp. on Ind. Electron.*, Seoul, 2009, pp. 1569-1574.

[21] M. Cirrincione, M. Pucci, G. Cirrincione, and G. -A. Capolino, "A new TLS-based MRAS speed estimation with adaptive integration for high-performance induction machine drives," *IEEE. Trans. Ind. Appl.*, vol. 40, no. 4, pp. 1116-1137, Jul./Aug. 2004.

[22] M. Cirrincione, and M. Pucci, "An MRAS-based sensorless high-performance induction motor drive with a predictive adaptive model," *IEEE. Trans. Ind. Electron.*, vol. 52, no. 2, pp. 532-551, Apr. 2005.

[23] M. Cirrincione, M. Pucci, G. Cirrincione, and G. -A. Capolino, "An adaptive speed observer based on a new total least-sqaures neuron for induction machine drives," *IEEE. Trans. Ind. Appl.*, vol. 42, no. 1, pp. 89-104, Jan./Feb. 2006.

[24] M. Cirrincione, M. Pucci, G. Cirrincione, and G. -A. Capolino, "Sensorless control of induction machines by a new neural algorithm: the new TLS EXIN neuron," *IEEE. Trans. Ind. Electron.*, vol. 54, no. 1, pp. 127-149, Feb. 2007.

[25] M. Cirrincione, M. Pucci, G. Cirrincione, and G. -A. Capolino, "Sensorless control of induction motors by reduced order observer with MCA EXIN + based adaptive speed estimation," *IEEE. Trans. Ind. Electron.*, vol. 54, no. 1, pp. 150-166, Feb. 2007.

[26] A. Accetta, M. Cirrincione, and M. Pucci, "TLS EXIN based neural sensorless control of a high dynamic PMSM," *Control Eng. Pract.*, vol. 20, no. 7, pp. 725-732, Jul. 2012

[27] G. Cirrincione, and M. Cirrincione, Neural-Based Orthogonal Data Fitting The EXIN Neural Networks. New York: Wiley, 2010.

[28] J. Pyrhönen, V. Hrabovcová, and R. S. Semken, Electrical Machine Drives Control An Introduction. New York: Wiley, 2016.